THE JOURNAL OF PHYSICAL CHEMISTRY A

Article

pubs.acs.org/JPCA

Effect of Concentration on the Formation of Rose Bengal Triplet State on Microcrystalline Cellulose: A Combined Laser-Induced Optoacoustic Spectroscopy, Diffuse Reflectance Flash Photolysis, and Luminescence Study

Yair Litman,[†] Matthew G. Voss,[†] Hernán B. Rodríguez,[†,‡] and Enrique San Román*[,†]

[†]INQUIMAE (UBA-CONICET)/DQIAyQF, Facultad de Ciencias Exactas y Naturales, Universidad de Buenos Aires, Ciudad Universitaria, Pab. II, Buenos Aires, Argentina

[‡]INIFTA (UNLP-CONICET), Facultad de Ciencias Exactas, Universidad Nacional de La Plata, Diag. 113 y Calle 64, La Plata, Argentina

ABSTRACT: Laser-induced optoacoustic spectroscopy (LIOAS), diffuse reflectance laser flash photolysis (DRLFP), and laser-induced luminescence (LIL) have been applied in conjunction to the determination of triplet state quantum yields of Rose Bengal (RB) supported on microcrystalline cellulose, a strongly light-scattering solid. Among the three used methods, the only one capable of providing absolute triplet quantum yields is LIOAS, but DRLFP and LIL aid in demonstrating that the LIOAS signal arises in fact from the triplet state and confirm the trend found with RB concentration. The coherence found for the three techniques demonstrates the usefulness of the approach. Observed triplet quantum yields are nearly constant within a limited concentration range, after which they decay strongly due to the generation of inactive dye aggregates or energy trapping centers. When quantum yields are divided by the fraction of absorbed light exciting the dye, the quotient falls off steadily with concentration, following the same trend as the observed fluorescence quantum yield. The conditions that maximize triplet formation are determined as a compromise between the rising light absorption and the decrease of quantum yield with RB concentration.

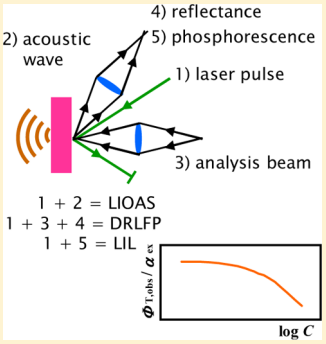

INTRODUCTION

Dye-modified solid materials are relevant to different areas, such as photosensitization and photocatalysis.[1,2] As a general rule, dyes with high triplet state quantum yields, Φ_T, are required for the development of photosensitizers based on the production of reactive oxygen species suited for photodynamic therapy and related applications. Though molecular photosensitizers are currently used, some applications, e.g., bacterial inactivation, can be favored by the use of heterogeneous systems composed of dyes bound to nanoparticles in suspension, microparticle beads, or immobilized films.[3−6]

Particulate materials have the advantage of offering high surface areas. Light scattering, typical of these materials, is also beneficial because the light path within the material is increased by multiple reflection and refraction. The increased light path also favors the reabsorption of fluorescence; excitation energy lost by emission is injected back into the system, thus repopulating the triplet state. For these and other reasons, observed fluorescence and triplet quantum yields, $\Phi_{F,obs}$ and $\Phi_{T,obs}$, defined in terms of the actual number of photons emitted and triplet molecules formed after fluorescence reabsorption, differ from the respective quantum yields of the isolated dye. Incorporation of dyes into inert solid matrixes may reduce dye aggregation and self-quenching compared to solution and increase photostability.[7] The study of the photophysics of these systems is difficult because light scattering adds complexity to experimental measurements, particularly when quantum yields are to be determined. Together with large excited state quantum yields, in order to improve the efficacy of materials, high light absorption rates are preferable, which in turn require large dye concentrations. In these conditions, however, deactivation of excited states by energy trapping becomes relevant.[8−10] Therefore, it is convenient to establish a practical range of concentrations ensuring substantial light absorption and Φ_T values as high as possible. We recently reviewed the effect of concentration on the photophysical properties of dyes in light scattering materials,[11] summarizing recent advances on their characterization, particularly on the evaluation of dye aggregation, inner filter effects, fluorescence quantum yields, and energy transfer and trapping efficiencies. A brief account was also made on the determination of triplet quantum yields by laser-induced optoacoustic spectroscopy (LIOAS).

Since the pioneering work of Schaap, Neckers, and others,[12,13] Rose Bengal (RB) was considered for the design of triplet state and singlet molecular oxygen generating

Special Issue: Current Topics in Photochemistry

Received: May 7, 2014
Revised: July 23, 2014
Published: August 11, 2014

   dx.doi.org/10.1021/jp5045095 | J. Phys. Chem. A 2014, 118, 10531−10537

materials both in solids and in soluble polymers.[14−16] We studied several years ago the fluorescence properties of RB in a microcrystalline cellulose matrix[17] and were able to determine recently $\Phi_{T,obs}$, in the same system using LIOAS,[18] showing that it remains nearly constant up to a concentration of 0.4 μmol (g cellulose)$^{-1}$. This fact was particularly intriguing because dye aggregation was observed in this concentration range. A negative dependence of $\Phi_{F,obs}$ was also found, though it was slight because dye dimers are luminescent. Also recently, we studied the phosphorescence and delayed fluorescence of various xanthene dyes on microcrystalline cellulose[19,20] using time-resolved methods, demonstrating concentration-independent phosphorescence decays and spectra in conditions where quenching of fluorescence takes place. The use of microcrystalline cellulose as a model support is convenient to study triplet states because dyes entrapped in the polymer matrix are protected from molecular oxygen quenching, thus allowing triplet state characterization without the need for sample degassing.[19,21−23]

In this work we extend the concentration range previously covered for RB on microcrystalline cellulose and incorporate other measurements to ascertain how $\Phi_{T,obs}$ depends on concentration. $\Phi_{T,obs}$ was evaluated by LIOAS, and results were checked by diffuse reflectance laser flash photolysis (DRLFP) and laser-induced luminescence (LIL) in the solid state. This work pursues two main objectives: (a) to evaluate any concentration dependence of $\Phi_{T,obs}$ in a broader range with respect to previous studies in order to establish a practical concentration range and (b) to check LIOAS results on the evaluation of $\Phi_{T,obs}$ for light-scattering solid materials by DRLFP and LIL measurements.

MATERIALS AND SAMPLE PREPARATION

RB disodic salt (Aldrich, 93%), Brilliant Blue G (BBG, Sigma-Aldrich), used as calorimetric reference for LIOAS measurements, and Rhodamine 101 inner salt (R101, Kodak), used as fluorescence reference, were used without further purification. Ethanol (Cicarelli, ACS grade) and microcrystalline cellulose powder (Aldrich, pH 5−7, average particle size 20 μm) were used also as received.

Dye and reference samples were prepared by suspending weighed amounts of cellulose (1.5 g), previously dried under vacuum at 40 °C during 48 h, in known amounts of a dye stock solution in ethanol, adding solvent to attain a final volume of 30 cm^3. The suspension was shaken for 5 min, and the solvent evaporated at low pressure in a Rotavap at 40 °C. Vacuum was regulated to attain solvent evaporation in ca. 15 min. In this way, samples bearing 0.021 to 4.22 μmol RB, 0.10 to 4.17 μmol BBG, and 1.10 to 1.70 μmol R101/g microcrystalline cellulose were prepared. Samples were dried in a vacuum at 40 °C for 48 h and maintained in the dark. Drying was repeated before reflectance, LIOAS, DRLFP, and LIL measurements. Measurements were performed at room temperature on optically thick and thin layers of each sample. A layer depth of 0.2 cm ensures optical thickness (no light transmission). Thin layers were prepared by spreading a small amount of sample on a double-sided adhesive tape fixed to a glass support.

METHODS

Total and diffuse reflectance spectra of optically thick solid layers were measured in a Shimadzu UV-3600 scanning spectrophotometer equipped with an integrating sphere. Barium sulfate was used as the reflectance reference. Measurements were performed by packing the sample into a suitable holder with a Plexiglas rod and releasing pressure before scanning. Steady-state emission spectra of optically thick layers were recorded on a PTI model QM-4 spectrofluorometer. Samples were measured in front face, placing a suitable optical filter in front of the detector to block excitation light. Spectra were corrected according to the dependence of the detection channel responsivity on wavelength obtained from the manufacturer and checked in our laboratory. The measurable quantity is $\Phi_{F,obs}$, defined as the number of emitted photons leaving the sample per photon absorbed by the system as a whole. Slight absorption by the supporting material and reabsorption and reemission of fluorescence render $\Phi_{F,obs}$ different from the true fluorescence quantum yield, Φ_F.[11] The relative method used for the determination of $\Phi_{F,obs}$ requires the knowledge of the absolute fluorescence quantum yield of the used reference, R101. The last quantity was determined using a method based on reflectance measurements with and without a suitable filter (Schott, BG38, 0.2 cm thickness) in front of the photodetector attached to the integrating sphere.[24] To obtain fluorescence spectra minimizing reabsorption, front face emission measurements were performed on thin layers of samples. For that sake, particles were spread onto one side of the adhesive tape and partially removed with a flat spatula until the shape of the emission spectrum remained constant. On conditioning samples for reflectance and fluorescence measurements, no special care other than drying was needed.

LIOAS probes were prepared by pressing 60 mg of dry solid samples into a specially designed aluminum holder at 25.5 bar for 120 s, yielding a probe thickness of 0.2 cm. Before LIOAS measurements the probes were allowed to relax at atmospheric pressure in a desiccator for at least 24 h. The LIOAS setup was described elsewhere,[25] and the principle underlying the technique is summarized in ref 11. The probe contained in the aluminum holder is illuminated from above with pulses from a Nd:YAG laser (Spectron, 8 ns @ 532 nm). Before reaching the sample, the laser beam passes through a set of two IR filters (Schott, KG5, 0.2 cm thickness) to avoid unwanted heating of the sample and spurious LIOAS signals, a gray wedge filter to obtain variable excitation energies, a pinhole, and a prism. The heat delivered by the sample develops an acoustic wave, which is converted into an electrical signal by a piezoelectric transducer. The first maximum of the electrical wave is the LIOAS signal, H (see Results and Discussion), from which quantum yields are calculated. As stated in ref 25, LIOAS signals depend on the experimental setup, which must remain unchanged during the whole set of measurements involving samples and references. The preparation of samples and references based on the same supporting material (microcrystallyne cellulose) conditioned in the same way and with the same dimensions and packing assures identical thermoelastic properties. The acoustic contact between sample holder and piezoelectric detector, mediated by a thick quartz plate, is ensured using silicone grease. The acoustic contact between sample and holder is regulated by pressing the sample against the holder with a Plexiglas plate maintained at a constant pressure among experiments. With all these precautions, LIOAS signals are reproducible within ±10%.

DRLFP and LIL experiments were performed using the same laser employed for LIOAS measurements. Optically thick samples were placed in a diffuse reflectance accessory inside a LP920 laser flash photolysis compartment (Edinburgh Instru-

ments). The analysis beam in DRLFP experiments was obtained from a horizontally driven Xe lamp (Osram XBO 150 W/1 OFR). It was focused on the sample surface overlapping the laser beam. Diffusely reflected light was collected avoiding as much as possible specular reflections of the analysis and laser beams and focused into the monochromator slit. A filter (Schott, OG550, 0.2 cm thickness) was placed in front of the sample to block unwanted wavelengths below 500 nm. The essentials of the technique are summarized elsewhere.[26] The scattered analyzing beam in DRLFP and emitted light in LIL experiments were detected on a PMT (Hamamatsu R929) after passing through appropriate filters and a computer controlled high throughput 1/4 m f/2.5 monochromator (Sciencetech 9055F) with dual 1200 l/mm diffraction gratings blazed at 450 and 700 nm. The PMT circuitry time constant was set to 2 μs, and the signal was digitized and fed into a PC using an ad hoc acquisition program for further analysis. To increase sensitivity, currently 32 traces were averaged. In these conditions, analysis lamp pulsing was unnecessary. As the dye and the supporting material are transparent at the phosphorescence emission wavelengths, phosphorescence is not reabsorbed by the sample, and its intensity is proportional to the number of triplet state dye molecules formed by the laser pulse.

The energy of the 532 nm laser pulse exciting the sample in LIOAS, DRLFP, and LIL experiments was measured using a Lab Master (Coherent, Ultima, Mod LM-P2) energy meter. The following energy ranges were used: 27 to 310 μJ for LIOAS, 10 to 2000 μJ for DRLFP, and 1.4 to 4200 μJ for LIL. The laser fluence at the sample surface can be calculated considering a spot area of 0.14 cm^2. Different filters and solutions of BBG in ethanol were used to obtain the desired energies. Analyzing wavelengths were 650 nm for DRLFP and 680 nm for LIL. In both cases the measurement at low laser pulse energies was required to correlate measured signals with $\Phi_{T,obs}$ (see Results and Discussion). Wavelengths were selected as a compromise between signal-to-noise ratio, interference of the laser beam, and, in the case of DRLFP, interference of phosphorescence and sample degradation, which took place at wavelengths near and below 400 nm. In the case of LIL experiments, the signal had its maximum at 680 nm, though the RB phosphorescence maximum lays at 737 nm[18] because of the steep decrease of the PMT responsivity at longer wavelengths. In both cases the diffraction grating blazed at 700 nm was used, and suitable cutoff filters (Schott, OG570, OG590, or RG610, 0.2 cm thickness) were set at the monochromator entrance. No detailed transient spectra were measured because the requirements cited above allowed spectral analysis to be performed only at low resolution between 600 and 700 nm.

RESULTS AND DISCUSSION

Thick layers were characterized by diffuse reflectance and fluorescence spectroscopy. Fluorescence spectra were measured also for thin layers. Reflectance spectra were transformed into remission function spectra, shown in Figure 1, according to

$$F(R) = \frac{(1-R)^2}{2R} \tag{1}$$

where R is the diffuse reflectance of an optically thick layer. The dye concentration in the samples is given in Table 1. The remission function, $F(R)$, would be proportional to the concentration of RB after subtraction of the spectrum of the supporting material if the absorption spectrum of the dye does not change with concentration. Inspection of the inset in Figure 1 shows that hypochromism is found at least for samples exceeding 1 μmol RB g^{-1}. This behavior was already observed in previous studies on microcrystallyne cellulose as a result of dye aggregation with formation of fluorescent dimers.[17,18] Thick and thin layer fluorescence spectra are shown in Figures 2 and 3, respectively. Typical effects of fluorescence reabsorption are observed in Figure 2: red-shift of the fluorescence maximum, increase of the relative height of the shoulder, and decrease of the spectrum area (see inset) as a function of concentration. Figure 3 shows that the first features are also evident for thin layers in excess of 0.2 μmol RB g^{-1}, showing that they are also affected by reabsorption. Notice, however, that the relative height of the shoulder is lower for thin layers. Fluorescence quantum yields, λ_{ex} = 525 nm, were calculated for optically thick samples through

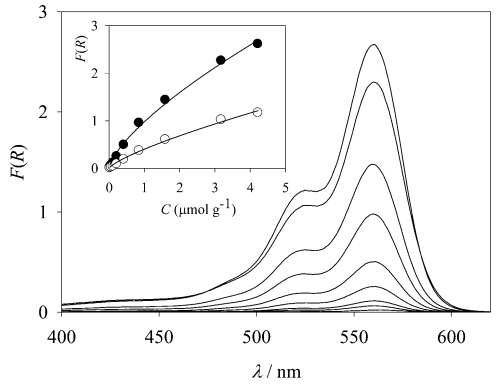

Figure 1. Remission function of samples RB1 to RB9 (bottom to top). Inset: remission function as a function of concentration at 563 nm (main maximum, black) and 526 nm (shoulder, white); full lines are fits to the potential equation $F(R) = aC^b$ without physical meaning.

$$\Phi_{F,obs} = \Phi^R_{F,obs}\frac{J(1-R^R_{t,ex})I^R_0}{J^R(1-R_{t,ex})I_0} \tag{2}$$

where J is the area below the fluorescence spectrum, $R_{t,ex}$ is the total reflectance at the excitation wavelength (525 nm), I_0 is the intensity of the excitation beam, and superscript R denotes reference (R101). $\Phi_{F,obs}$ values are shown in Table 1 as a function of concentration.

LIOAS signals, H, were measured as a function of the laser pulse energy, E, for thick layers of samples as described in the experimental section, and $\Phi_{T,obs}$ values were obtained from

$$\frac{H}{E} = A(1-R_{t,ex})\left(1 - \Phi_{F,obs}\frac{\langle\bar{\nu}_F\rangle}{\bar{\nu}_0} - \Phi_{T,obs}\frac{E_T}{hc\bar{\nu}_0}\right) \tag{3}$$

where A is a function of system geometry and thermoelastic properties of the sample, $R_{t,ex}$ is the total reflectance at the excitation wavelength, 532 nm in this case, $\langle\bar{\nu}_F\rangle = \int\bar{\nu}_F f(\bar{\nu}_F)d\bar{\nu}_F$ is the fluorescence average wavenumber, $f(\bar{\nu}_F)$ in the area normalized observed thick layer fluorescence spectrum, $\bar{\nu}_0$ is the excitation frequency, E_T is the triplet energy, h is Planck's constant, and c is the speed of light in vacuum. The value of A is obtained from the same equation applied to a calorimetric reference with $\Phi_{F,obs}$ = 0 and $\Phi_{T,obs}$ = 0 (BBG) on the same supporting matrix and with the same geometry as the sample. Results are reported in Table 1.

dx.doi.org/10.1021/jp5045095 | J. Phys. Chem. A 2014, 118, 10531−10537

Table 1. Summary of Quantum Yield Results[a]

	C (μmol g^{-1})	α_{ex} (525 nm)	$\Phi_{F,obs}$ (525 nm)	$R_{t,ex}$ (532 nm)	α_{ex} (532 nm)	$\Phi_{T,obs}$ (LIOAS)	rel.$\Phi_{T,obs}$ (DRLFP)	rel.$\Phi_{T,obs}$ (LIL)
RB1	0.021	0.68		0.87	0.67			
RB2	0.056	0.86	0.070	0.81	0.86	0.44	0.00125	0.0189
RB3	0.108	0.92	0.061	0.75	0.92	0.47	0.00126	0.0187
RB4	0.214	0.97	0.058	0.66	0.97	0.49	0.00118	0.0192
RB5	0.420	0.98	0.058	0.56	0.98	0.46	0.00122	0.0193
RB6	0.850	0.99	0.042	0.45	0.99	0.29	0.00112	0.0160
RB7	1.597	0.99	0.034	0.33	0.99	0.36	0.00098	0.0114
RB8	3.179	1.00	0.018	0.29	1.00	0.04	0.00038	0.0052
RB9	4.222	1.00	0.021	0.23	1.00	0.12	0.00062	0.0069

[a] $\alpha_{ex} = [F(R) - F(R)_{cellulose}]/F(R)$; $R_{t,ex}$, total reflectance at excitation wavelength; rel. means relative; see text for remaining symbols.

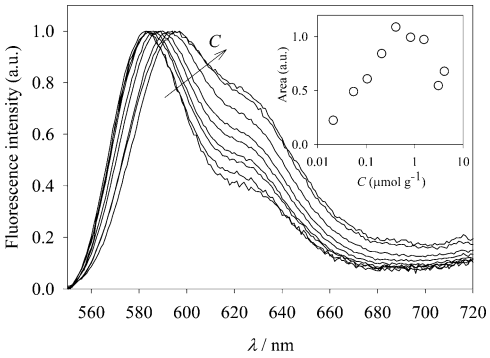

Figure 2. Normalized fluorescence intensity of thick layers of samples RB1 to RB9 (λ_{ex} = 525 nm); cellulose background subtracted. Inset: area of the fluorescence spectra as a function of concentration.

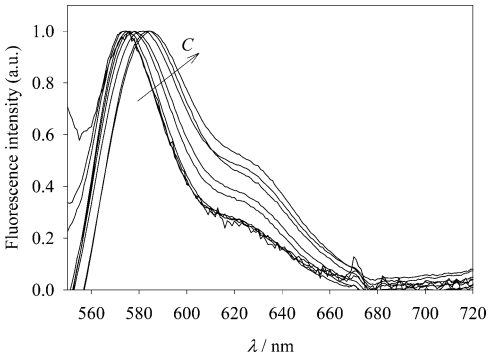

Figure 3. Normalized fluorescence intensity of thin layers of samples RB1 to RB9 (λ_{ex} = 525 nm); cellulose background subtracted.

The triplet−triplet spectrum of RB has a band superimposed to the ground state absorption spectrum, leading to complex photophysics at 532 nm[27] and another one peaking at 1020 nm.[28,29] DRLFP and LIL studies were performed to ensure that the measured quantity is in fact $\Phi_{T,obs}$. This confirmation is worthwhile because LIOAS alone does not allow a characterization of the observed long-lived species. According to Kessler et al.,[30] the number of molecules of the transient species followed by DRLFP is proportional to

$$S(t) = \frac{R_0 - R(t)}{R_0} \quad (4)$$

when $R_0 - R(t) < 0.1$, where $R(t)$ is the diffuse reflectance of the sample at the analyzing wavelength at time t, and R_0 is the diffuse reflectance at the same wavelength before the laser pulse. Reflectances are proportional to the voltage across the PMT anode. Alternatively, the triplet state can be followed measuring its luminescence as a function of time in the absence of analyzing light. Results are shown for selected samples in Figure 4. DRLFP measurements were performed at the onset of

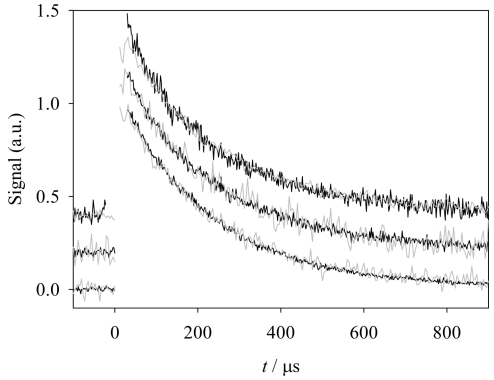

Figure 4. LIL (black) and DRLFP (gray) signals as a function of time for samples RB3, RB6, and RB9 (bottom to top). Traces are averages of several experiments. DRLFP signals were measured at 650 nm with laser energies between 10 and 2000 μJ; LIL signals at 680 nm and laser energies between 4 and 16 μJ. For clarity, traces corresponding to samples RB6 and RB9 are displaced 0.2 and 0.4 units, respectively.

the triplet−triplet absorption band in the visible and are contaminated with nearly 3% luminescence. DRLFP and LIL traces are multiexponential and overlap within the experimental noise, showing that the measured signals correspond to the same species, namely, the triplet state of RB. Traces corresponding to samples at different concentrations from RB1 to RB9 also overlap (not shown), implying that the triplet decay is independent of concentration, as already found for eosin Y[20] and phloxine B[19] on microcrystalline cellulose. Triplet−triplet annihilation can also be safely excluded. Because of the experimental restrictions quoted at the end of the Methods section, it was not possible to recover the triplet state and the phosphorescence spectrum, which should be a combination of spectra in different environments, decaying with different lifetime distributions as observed for eosin Y.[20]

Figure 5 shows DRLFP and LIL signals extrapolated to $t = 0$ as a function of E for laser pulse energies greater than 10 μJ. At very high energies, saturation should in principle take place if the background absorbs at the excitation wavelength. This limit is not reached under the experimental conditions. It may be seen that DRLFP and LIL experiments show the same behavior, which may be accurately represented by the empirical hyperbolic equation signal$(t = 0) = aE/(b + E) + cE$, demonstrating again that the species followed in both cases is the same.

dx.doi.org/10.1021/jp5045095 | J. Phys. Chem. A 2014, 118, 10531−10537

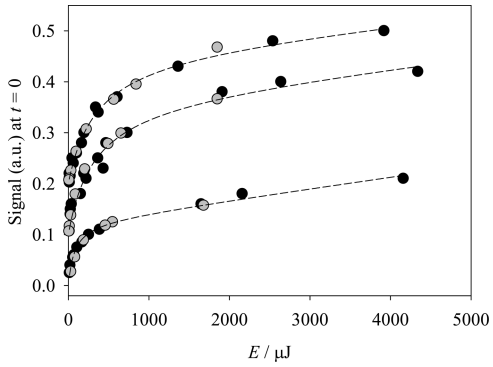

Figure 5. LIL (black) and DRLFP (gray) signals at $t = 0$ as a function of the laser energy for samples RB3, RB6, and RB9 (bottom to top). For clarity, curves corresponding to samples RB6 and RB9 are displaced 0.1 and 0.2 units, respectively. Full lines are fits to a hyperbolic equation without physical meaning. DRLFP signals were measured at 650 nm and LIL signals at 680 nm.

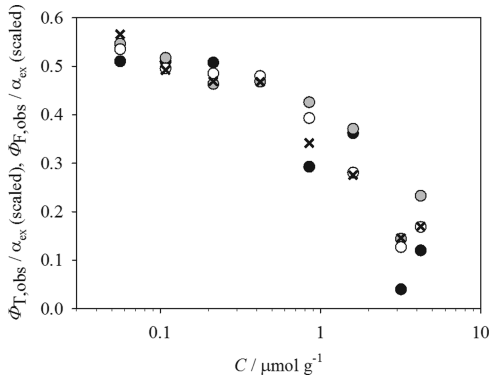

Figure 6. Observed triplet quantum yields divided by α_{ex} (λ_{ex} = 532 nm) obtained by LIOAS (black circles), DRLFP (gray circles), and LIL (white circles) and observed fluorescence quantum yields divided by α_{ex} (λ_{ex} = 525 nm, ×) as a function of concentration. Relative triplet quantum yields obtained by DRLFP and LIL and fluorescence quantum yields are scaled to match the absolute quantum yields obtained by LIOAS at the lowest concentrations (see text).

From signals extrapolated at $t = 0$, relative $\Phi_{T,obs}$ values can be gathered. For this sake, laser excitation should be weak enough to ensure linearity with pulse energy. This condition is met when the dye ground state is negligibly depleted by the laser pulse. In that case, the triplet state acquires an exponential profile across the sample.[31,32] The number of triplet molecules can then be related to the laser pulse energy through[30]

$$N_T = \frac{E\lambda_{ex}}{hc}(1 - R_{t,ex})\Phi_{T,obs} \quad (5)$$

where all symbols have the same meaning as in eq 3. Therefore, the slope of the DRLFP signal (eq 4) or the phosphorescence signal extrapolated to $t = 0$ as a function of E in the linear region divided by $(1 - R_{t,ex})$ is proportional to $\Phi_{T,obs}$. For LIL experiments, linearity was found for laser pulse energies lower than 130 μJ. DRLFP measurements were noisier, and the number of points below 130 μJ scarce, so that slopes were calculated using the fitting hyperbolic equation (see Figure 5). Relative $\Phi_{T,obs}$ values calculated by both methods are shown in Table 1. Inspection of the table shows that $\Phi_{T,obs}$ measured by the three used methods is almost constant in average up to 0.42 μmol g^{-1} and decreases at higher concentrations, whereas $\Phi_{F,obs}$ decreases slowly in the whole concentration range. $\Phi_{F,obs}$ values are in line with those measured earlier in a narrower concentration range[17,18] (though they are somewhat larger in the last reference). A deeper insight can be gained by dividing quantum yields by the fraction of incident radiation exciting the dye, α_{ex} (see Table 1), to correct them by the absorption of impurities in microcrystalline cellulose at the excitation wavelength, particularly at the smallest RB concentrations. Figure 6 shows $\Phi_{T,obs}/\alpha_{ex,532\ nm}$ and $\Phi_{F,obs}/\alpha_{ex,525\ nm}$ as a function of the concentration of RB. To allow comparison, quotients corresponding to fluorescence and DRLFP and LIL signals were scaled to match absolute values measured by LIOAS. Scaling was afforded forcing the averages of the quotients corresponding to samples RB2 to RB5 to coincide with those obtained by LIOAS. It is clearly seen in Figure 6 that $\Phi_{T,obs}/\alpha_{ex}$ and $\Phi_{F,obs}/\alpha_{ex}$ are both slow decreasing functions of C in the whole concentration range (notice that the abscissa is logarithmic). The decrease of $\Phi_{F,obs}/\alpha_{ex}$ can be attributed to fluorescence reabsorption and dye aggregation. Formation of fluorescent dimers with lower Φ_F than monomers slows down somewhat the decrease at low concentrations, whereas at concentrations in excess of 0.4 μmol g^{-1} higher order, probably dark, aggregates are formed,[17] leading to a parallel decrease of $\Phi_{F,obs}/\alpha_{ex}$ and $\Phi_{T,obs}/\alpha_{ex}$. The low value of the fluorescence quantum yield determines that the enhancement of $\Phi_{T,obs}$ by fluorescence reabsorption should be negligible.

Inspection of Table 1 shows that a practical concentration range for the generation of triplet states from RB supported on microcrystalline cellulose at λ_{ex} = 532 nm may be set around 0.1 to 0.4 μmol g^{-1}. This is the concentration range that maximizes $\Phi_{T,obs} \times (1 - R_{t,ex})$. The maximum arises from a compromise between $\Phi_{T,obs}$, decreasing with dye aggregation and/or excitation energy trapping, and the fraction of incident radiation absorbed by the sample, increasing with RB loading. Working at different wavelengths changes the maximum of the above product but does not change the optimum concentration range provided that the cellulose matrix does not increase its absorption. The best results would be obtained working near the RB absorption maximum (see Figure 1).

The determination of triplet quantum yields in solid systems by alternative methods has been reported in the literature. Schtosser et al. used EPR and paramagnetic standards to obtain absolute triplet quantum yields of aromatic compounds in transparent ethanol glasses at 77 K.[33] Light absorption was determined by actinometry, a method that cannot be employed in our present conditions owing to light scattering, which cannot be modeled so easily in an EPR cell. Another interesting approach is that of King et al.[34] These authors determine the ground state recovery after femtosecond excitation in the subnanosecond and millisecond scales. The ratio between the slow and total recovery amplitudes allows determination of triplet quantum yields without resource to any measurement of the number of triplet molecules and absorbed photons. This technique was applied to low light scattering polymer films and can be in principle applied to thin layers of samples, though heterogeneity can be a highly complicating factor. Of course, working simultaneously at very different time scales requires special conditions to be met.

LIOAS has been demonstrated itself as a powerful technique for the determination of $\Phi_{T,obs}$ absolute values for light scattering materials as long as optically thick samples are used. However, this method alone cannot ensure that the observed state is the triplet one. DRLFP and LIL, though yielding relative

dx.doi.org/10.1021/jp5045095 | J. Phys. Chem. A 2014, 118, 10531−10537

values, can be used as complementary techniques because the corresponding signals can be set to the linear regime at enough low laser pulse energies or using good extrapolation functions. Of course, working at the low energy DRLFP limit requires a very good instrumental sensitivity to be achieved. In this work, sensitivity was privileged against working at different wavelengths in order to characterize the excited state by its absorption spectrum. The objective was fulfilled by using phosphorescence as a specific triplet follower. The coherence found for the three techniques shown in Figure 6 demonstrates the usefulness of the approach. In case of non or weakly phosphorescing dyes, DRLFP alone can be used. To our knowledge, this is the first time DRLFP has been used to assess relative triplet quantum yields without ad hoc assumptions.

AUTHOR INFORMATION

Corresponding Author

*(E.S.R.) E-mail: esr@qi.fcen.uba.ar. Tel: +5411-4576-3378, ext. 118. Fax: +5411-4576-3341.

Notes

The authors declare no competing financial interest.

ACKNOWLEDGMENTS

This work has been supported by the University of Buenos Aires, the National Research Council of Argentina (CONICET), and the Agencia Nacional de Promoción Científica y Tecnológica (ANPCyT). H.B.R. and E.S.R. are staff members of CONICET. Y.L. acknowledges a fellowship from the Consejo Interuniversitario Nacional (CIN). Generous funding from Caltech and the Rose Hills Summer Undergraduate Research Fellowship (SURF) programmes covered the travel and stay of M.G.V. and part of the budget of the project.

REFERENCES

(1) Ronzani, F.; Saint-Cricq, P.; Arzoumanian, E.; Pigot, T.; Blanc, S.; Oelgemöller, M.; Oliveros, E.; Richard, C.; Lacombe, S. Immobilized Organic Photosensitizers with Versatile Reactivity for Various Visible-Light Applications. *Photochem. Photobiol.* **2014**, *90*, 358−368.

(2) Ishii, K. Functional Singlet Oxygen Generators Based on Phthalocyanines. *Coord. Chem. Rev.* **2012**, *256*, 1556−1568.

(3) Bonnett, R.; Krysteva, M. A.; Lalov, I. G.; Artarsky, S. V. Water Disinfection Using Photosensitizers Immobilized on Chitosan. *Water Res.* **2006**, *40*, 1269−1275.

(4) Benabbou, A. K.; Guillard, C.; Pigeot-Rémy, S.; Cantau, C.; Pigot, T.; Lejeune, P.; Derriche, Z.; Lacombe, S. Water Disinfection Using Photosensitizers Supported on Silica. *J. Photochem. Photobiol., A* **2011**, *219*, 101−108.

(5) Jiménez-Hernández, M. E.; Manjón, F.; García-Fresnadillo, D.; Orellana, G. Solar Water Disinfection by Singlet Oxygen Photogenerated with Polymer-Supported Ru(II) Sensitizers. *Sol. Energy* **2006**, *80*, 1382−1387.

(6) Guo, Y.; Rogelj, S.; Zhang, P. Rose Bengal-Decorated Silica Nanoparticles as Photosensitizers for Inactivation of Gram-Positive Bacteria. *Nanotechnology* **2010**, *21*, 065102.

(7) Avnir, D.; Levy, D.; Reisfeld, R. The Nature of the Silica Cage as Reflected by Spectral Changes and Enhanced Photostability of Trapped Rhodamine 6G. *J. Phys. Chem.* **1984**, *88*, 5956−5959.

(8) Knoester, J.; Van Himbergen, J. E. (1987) On the Theory of Concentration Selfquenching by Statistical Traps. *J. Chem. Phys.* **1987**, *86*, 3571−3576.

(9) Rodríguez, H. B.; San Román, E. Excitation Energy Transfer and Trapping in Dye-Loaded Solid Particles. *Ann. N.Y. Acad. Sci.* **2008**, *1130*, 247−252.

(10) Shi, W.-J.; Barber, J.; Zhao, Y. Role of Formation of Statistical Aggregates in Chlorophyll Fluorescence Concentration Quenching. *J. Phys. Chem. B* **2013**, *117*, 3976−3982.

(11) Rodríguez, H. B.; San Román, E. Effect of Concentration on the Photophysics of Dyes in Light Scattering Materials. *Photochem. Photobiol.* **2013**, *89*, 1273−1282.

(12) Blossey, E. C.; Neckers, D. C.; Thayer, A. L.; Schaap, A. P. Polymer-Based Sensitizers for Photooxidations. *J. Am. Chem. Soc.* **1973**, *95*, 5820−5822.

(13) Schaap, A. P.; Thayer, A. L.; Blossey, E. C.; Neckers, D. C. Polymer Based Sensitizers for Photooxidations. II. *J. Am. Chem. Soc.* **1975**, *97*, 3741−3745.

(14) Paczkowski, J.; Neckers, D. C. Polymer-Based Sensitizers for the Formation of Singlet Oxygen. New Studies of Polymeric Derivatives of Rose Bengal. *Macromolecules* **1985**, *18*, 1245−1253.

(15) Nowakowska, M.; Kępczyński, M.; Szczubialka, K. New Polymeric Photosensitizers. *Pure Appl. Chem.* **2001**, *73*, 491−495.

(16) Nakonechny, F.; Pinkus, A.; Hai, S.; Yehosha, O.; Nitzan, Y.; Nisnevitch, M. Eradication of Gram-Positive and Gram-Negative Bacteria by Photosensitizers Immobilized in Polystyrene. *Photochem. Photobiol.* **2013**, *89*, 671−678.

(17) Rodríguez, H. B.; Lagorio, M. G.; San Román, E. Rose Bengal Adsorbed on Microgranular Cellulose: Evidence on Fluorescent Dimers. *Photochem. Photobiol. Sci.* **2004**, *3*, 674−680.

(18) Tomasini, E. P.; Braslavsky, S. E.; San Román, E. Triplet Quantum Yields in Light-Scattering Powder Samples Measured by Laser-Induced Optoacoustic Spectroscopy (LIOAS). *Photochem. Photobiol. Sci.* **2012**, *11*, 1010−1017.

(19) Duarte, P.; Ferreira, D. P.; Ferreira Machado, I.; Vieira Ferreira, L. F.; Rodríguez, H. B.; San Román, E. Phloxine B as a Probe for Entrapment in Microcrystalline Cellulose. *Molecules* **2012**, *17*, 1602−1616.

(20) Rodríguez, H. B.; San Román, E.; Duarte, P.; Ferreira Machado, I.; Vieira Ferreira, L. F. Eosin Y Triplet State as a Probe of Spatial Heterogeneity in Microcrystalline Cellulose. *Photochem. Photobiol.* **2012**, *88*, 831−839.

(21) Murtagh, J.; Thomas, J. K. Effect of Humidity and Temperature on Photoinduced Reactions in Cellulose. *Chem. Phys. Lett.* **1988**, *148*, 445−451.

(22) Vieira Ferreira, L. F.; Netto-Ferreira, J. C.; Khmelinskii, I. V.; Garcia, A. R.; Costa, S. M. B. Photochemistry on Surfaces: Matrix Isolation Mechanisms Study of Interactions of Benzophenone Adsorbed on Microcrystalline Cellulose Investigated by Diffuse Reflectance and Luminescence Techniques. *Langmuir* **1995**, *11*, 231−236.

(23) Sikorski, M.; Wilkinson, F.; Bourdelande, J. L.; Gonzalez Moreno, R.; Steer, R. P. Triplet States of Aromatic Thioketones Supported on Cellulose. *Phys. Chem. Chem. Phys.* **1999**, *1*, 3639−3645.

(24) Mirenda, M.; Lagorio, M. G.; San Román, E. Photophysics on Surfaces: Determination of Absolute Fluorescence Quantum Yields from Reflectance Spectra. *Langmuir* **2004**, *20*, 3690−3697.

(25) Tomasini, E. P.; San Román, E.; Braslavsky, S. E. Validation of Fluorescence Quantum Yields for Light-Scattering Powdered Samples by Laser-Induced Optoacoustic Spectroscopy. *Langmuir* **2009**, *25*, 5861−5868.

(26) Wilkinson, F.; Kelly, G. Diffuse Reflectance Flash Photolysis. In *Handbook of Organic Photochemistry*; Scaiano, J. C., Ed.; CRC Press: Boca Raton, FL, 1989; Vol. *1*, Chapter 12.

(27) Lambert, C. R.; Kochevar, I. E.; Redmond, R. R. Differential Reactivity of Upper Triplet States Produces Wavelength-Dependent Two-Photon Photosensitization Using Rose Bengal. *J. Phys. Chem. B* **1999**, *103*, 3737−3741.

(28) Islam, S. D.-M.; Ito, O. Solvent Effects on Rates of Photochemical Reactions of Rose Bengal Triplet State Studied by Nanosecond Laser Photolysis. *J. Photochem. Photobiol., A* **1999**, *123*, 53−59.

(29) Gratz, H.; Penzkofer, A. Triplet−Triplet Absorption of Some Organic Molecules Determined by Picosecond Laser Excitation and

Time-Delayed Picosecond Light Continuum Probing. *J. Photochem. Photobiol., A* **1999**, *127*, 21−30.
(30) Kessler, R. W.; Krabichler, G.; Uhl, S.; Oelkrug, D.; Hagan, W. P.; Hyslop, J.; Wilkinson, F. Transient decay Following Pulse Excitation of Diffuse Scattering Samples. *Opt. Acta* **1983**, *8*, 1099−1111.
(31) Lin, T.-P.; Kan, H. K. A. Calculation of Reflectance of a Light Diffuser with Nonuniform Absorption. *J. Opt. Soc. Am.* **1970**, *60*, 1252−1260.
(32) Oelkrug, D.; Honnen, W.; Wilkinson, F.; Willsher, C. Modelling of Transient Production and Decay Following Laser Excitation of Opaque Materials. *J. Chem. Soc., Faraday Trans. 2* **1987**, *83*, 2081−2095.
(33) Shtosser, R.; Pergushov, V. I.; Gurman, V. S. Quantum Yields of Formation of Triplet States of Certain Aromatic Molecules in the Solid Phase at 77 K Determined by ESR. *Theor. Exp. Chem.* **1984**, *20*, 458−462.
(34) King, S. M.; Rothe, C.; Dai, D.; Monkman, A. P. Femtosecond Ground State Recovery: Measuring the Intersystem Crossing. *J. Chem. Phys.* **2006**, *124*, 234903.